MOLECULAR AND CELLULAR BIOLOGY, Feb. 2009, p. 726–735 Vol. 29, No. 3
0270-7306/09/$08.00+0 doi:10.1128/MCB.01180-08

Protein Kinase KIS Localizes to RNA Granules and Enhances Local Translation[▽]

Serafí Cambray,‡ Neus Pedraza,‡ Marta Rafel, Eloi Garí, Martí Aldea, and Carme Gallego*

Departament de Ciències Mèdiques Bàsiques, IRBLLEIDA, Universitat de Lleida, Montserrat Roig, 2, 25008 Lleida, Catalonia, Spain

Received 26 July 2008/Returned for modification 22 August 2008/Accepted 10 November 2008

The regulation of mRNA transport is a fundamental process for cytoplasmic sorting of transcripts and spatially controlled translational derepression once properly localized. There is growing evidence that translation is locally modulated as a result of specific synaptic inputs. However, the underlying molecular mechanisms that regulate this translational process are just emerging. We show that KIS, a serine/threonine kinase functionally related to microtubule dynamics and axon development, interacts with three proteins found in RNA granules: KIF3A, NonO, and eEF1A. KIS localizes to RNA granules and colocalizes with the KIF3A kinesin and the β-actin mRNA in cultured cortical neurons. In addition, KIS is found associated with KIF3A and 10 RNP-transported mRNAs in brain extracts. The results of knockdown experiments indicate that KIS is required for normal neurite outgrowth. More important, the kinase activity of KIS stimulates 3′ untranslated region-dependent local translation in neuritic projections. We propose that KIS is a component of the molecular device that modulates translation in RNA-transporting granules as a result of local signals.

There are two important reasons why proteins are localized through their mRNAs rather than directly. First, mRNA localization not only targets the protein to the correct region of the cell but also prevents its expression elsewhere. The second reason for localizing a protein through its mRNA is that it devolves the control of protein expression to individual regions of the cytoplasm. This allows a cell to respond rapidly to a local requirement for the protein and makes it possible to regulate gene expression independently in different subcompartments of the cell (21, 32, 37). These factors are particularly important in large and highly polarized cells, such as neurons, where translation of localized mRNAs in growth cones seems to be important for axon guidance, whereas local control of protein synthesis in dendrites contributes to synaptic plasticity (6, 36). Localized mRNAs are usually transported in large ribonucleoprotein particles (RNPs), which have been referred to as RNA granules. It is thought that this structure serves to prevent premature mRNA translation/degradation during transport and that mRNAs might be released into a translationally competent form by locally originated signals (23, 33). RNPs vary in composition and include multiple mRNAs, ribosomes, and regulatory proteins, as well as molecular-motor proteins (2). Two studies using different approaches have attempted a molecular characterization of RNPs isolated from neural tissue. The first study used kinesin KIF5A in an affinity purification approach and identified a large number of proteins in granules from the adult mouse brain, including known regulators of mRNA transport (Purα and Staufen1) and eukaryotic translation factors (eIF2A and eEF1A), as well as CaMKIIα and Arc mRNAs (19). The second study (9) isolated a fraction enriched in RNPs from embryonic rat brains and demonstrated the presence of the β-actin mRNA and dynein as a motor protein. Nevertheless, the two RNP preparations had many common components, including several heterogeneous nuclear ribonucleoproteins (hnRNPs), SYNCRIP, FMRP, Purα, Staufen1, and RNA helicases. Finally, Tau mRNA and kinesin protein 3A (KIF3A) have been found associated in P19 neurons in culture (3). Recently, a great deal of research has focused on the regulation of dendritic mRNA translation in neurons, addressing two distinct questions: first, how are mRNAs transported into dendrites, and second, how is the translation of these mRNAs regulated? It is now clear that both processes involve mRNA-binding proteins that are primarily bound to the 3′ untranslated region (UTR) of responsive mRNAs (35). The best-studied examples are the *trans*-acting factors ZBP1 and CPEB1, which bind a 54-nucleotide (nt) sequence in the 3′ UTR of β-actin mRNA and a 170-nt sequence in the 3′ UTR of CaMKIIα mRNA, respectively, with both interactions required for proper mRNA localization and translational inhibition (16, 17, 30).

KIS was first identified as a *k*inase that *i*nteracts with *s*tathmin (28), a phosphoprotein that controls microtubule dynamics with a role in axon development (39). On the other hand, KIS has been described as a negative regulator of the Cdk inhibitor $p27^{KIP1}$, thus promoting cell cycle progression in a fibroblast line (5). Finally, Manceau et al. (29) have shown in vitro that KIS phosphorylates the splicing factor SF1 on two adjacent SP motifs and enhances the formation of the SF1-$U2AF^{65}$-RNA ternary complex, which suggests that KIS may participate in RNA splicing. Here, we show that KIS interacts with KIF3A, NonO, and eEF1A, three proteins found in RNA granules; colocalizes with KIF3A kinesin in neurites; and is important for neurite outgrowth. Furthermore, KIS associates with the RNP-transported mRNAs and stimulates translation driven by the β-actin 3′ UTR, suggesting that KIS could help

* Corresponding author. Mailing address: Departament de Ciències Mèdiques Bàsiques, IRBLLEIDA, Universitat de Lleida, Montserrat Roig, 2, 25008 Lleida, Catalonia, Spain. Phone: 34 973702438. Fax: 34 973702426. E-mail: carme.gallego@cmb.udl.cat.

‡ S.C. and N.P. contributed equally to this work.

▽ Published ahead of print on 17 November 2008.

activate the translation of specific mRNAs by locally originated signals.

MATERIALS AND METHODS

Cortical-cell culture, expression vectors, and siRNAs. Cerebral cortices of embryonic day 14 mouse embryos were dissociated and cultured in neurobasal medium (Gibco) plus 1% N2, 2% B27, 0.5 mM L-glutamine, and 20 ng/ml brain-derived neurotrophic factor (BDNF) (Preprotech) on polylysine-laminin-coated plates or glass coverslips at 75,000 cells/cm^2. The medium was replaced every 2 days. *Mus musculus* KIS (IMAGE ID, 6414877) fused to three copies of the FLAG or hemagglutinin (HA) epitope was cloned under the cytomegalovirus promoter in a lentiviral vector derived from pDSL (Invitrogen) by removing the green fluorescent protein (GFP) transcriptional unit. Tagged versions (FLAG or HA) of KIF3A (obtained from two-hybrid experiments) and KIS were also cloned into pcDNA3 (Invitrogen). The KIS kinase-dead K54A mutant (K54^{KD}) (5) was generated using CGCCCTTGCGCAGTTCCTGCCTCC (the mutation is underlined) and GCAGGAAAGAACCGGTGAGCAAAAGG as mutation and selection primers, respectively, and the Transformer Site-Directed Mutagenesis kit (Clontech). KIS and KIS^{KD} were cloned into the DsRed vector (Clontech) to obtain red-fluorescent derivatives. To obtain myr-dGFP$^{Actb\text{-}3'UTR}$ (see below), a Cdk5 myristoylation signal (MGTVLSLSPSY) was added to the forward primer (CGCGAGATCTATGGGCACGGTGCTGTCCCTGTCTCCCA GCTACGCCCAGTCCAAGCACGGCCT) during amplification of the destabilized *Zoanthus* sp. GFP sequences (Clontech). The final pcDNA3 derivatives contained the zipcode sequence from the 3′ UTR of β-actin (nt 1208 to 1264; NM_007393). Purified small interfering RNA (siRNA) duplexes (Sigma-Proligo) were as described previously (5) and contained the following sequences: mouse KIS, GCAGUUCCUGCCUCCGGGAdTdT, and control, CUUACGCUGAG UACUUCGAdTdT. Transfection of cortical neurons was performed 3 days after plating them with Lipofectamine 2000 (Invitrogen). Details of all constructs are available upon request.

Lentivirus production and infection. HEK293T cells were transfected with Lipofectamine 2000 (Invitrogen) with equal amounts of lentiviral expression vector, envelope plasmid pVSV.G, and packaging plasmid pHR′82ΔR and cultured in neurobasal medium supplemented as described above. The lentiviruses were harvested 3 days after transfection, filtered through 0.45-μm cellulose acetate syringe filters, and diluted 1:1 in fresh neurobasal medium with supplements before use. Cortical cells were infected during plating, and the medium was replaced after 2 days.

Yeast two-hybrid screens. Full-length mouse KIS was fused to the Gal4 DNA-binding domain in pGBKT7, transformed into AH109 (*MAT***a** trp1-901 leu2-3,112 ura3-52 his3-200 *gal4*Δ *gal80*Δ *LYS2*::*GAL1*$_{UAS}$-*GAL1*$_{TATA}$-*HIS3 GAL2*$_{UAS}$-*GAL2*$_{TATA}$-*ADE2 URA3*::*MEL1*$_{UAS}$-*MEL1*$_{TATA}$-*lacZ MEL1*), and used as bait to screen an embryonic day 11 mouse embryo cDNA library in pGADT7-Rec (Clontech) and an adult mouse brain cDNA library in pACT2 (Clontech) following the instructions given by the manufacturer. Positive clones were identified on plates lacking leucine, tryptophan, and histidine with 25 mM 3-aminotriazole.

Immunoprecipitations, immunoblotting, and real-time reverse transcription (RT)-PCR analysis. HEK293T cells were harvested 24 h after transfection with the appropriate plasmids. Cells were resuspended in lysis buffer (20 mM HEPES, pH 7.9, 125 mM NaCl, 0.1% Triton X-100, 1 mM EDTA, phosphatase inhibitors, 1 mM phenylmethylsulfonyl fluoride, and protease inhibitors), and extracts were sonicated on ice and spun for 10 min at 14,000 rpm. The supernatants were added to 50 μl of anti-FLAG-agarose (M2; Sigma), and samples were rocked for 2 h at 4°C. The beads were collected by centrifugation (1 min at 2,000 rpm), washed three times with 1 ml of cold lysis buffer, and finally resuspended in loading buffer, boiled, and loaded onto sodium dodecyl sulfate-polyacrylamide gel electrophoresis gels.

The immunoprecipitation protocol applied to mouse brain extracts was as described previously (10). Endogenous KIS protein was immunoprecipitated from 1.5 ml of brain extract (protein concentration, 30 mg/ml) with 40 μl of αKIS antiserum (Isogen Life Science, Maarssen, Holland) raised against the DYLEN EDEYEDVVEDVKEE peptide as described previously (5). The same protocol was adapted to immunoprecipitate FLAG-KIS complexes from cortical neurons. Briefly, neurons infected with a lentivirus expressing FLAG-KIS and cultured for 7 days were homogenized in lysis buffer (20 mM HEPES, pH 7.4, 150 mM NaCl, 5 mM $MgCl_2$, 0.5% Triton X-100, 1 mM dithiothreitol supplemented with 1 mM phenylmethylsulfonyl fluoride, protease inhibitors, and 100 U/ml RNase inhibitor [Invitrogen]). Following two rounds of centrifugation (10 min at 1,000 × *g* and 10 min at 10,000 × *g*), the supernatant was incubated with 50 μl of anti-FLAG-agarose (M2; Sigma) preblocked for 1 h with 0.2% bovine serum albumin, 0.5 mg/ml tRNA in lysis buffer. Samples were rocked at 4°C overnight and subjected to five 30-min washes with lysis buffer with 250 mM NaCl.

Proteins were transferred to polyvinylidene difluoride membranes (Millipore), and the primary antibodies used in detection steps were against whole KIS (1:50; polyclonal; produced in collaboration with AbBCN), HA (1:2,500; monoclonal 12CA5; our own ascitic fluid stocks), FLAG (1:200; polyclonal F7425; Sigma), NonO (1:1,000; monoclonal 3; BD Transduction Laboratory), KIF3A (1:250; monoclonal 28; BD Transduction Laboratory), eEF1A (1:200; monoclonal CBP-KK1; Upstate Biotechnology), PSF (pyrimidine tract binding protein-associated splicing factor) (1:1,000; monoclonal B92; Sigma), tubulin (1:2,000;, monoclonal DM1A; Sigma), and hnRNP A2/B1/B2 (1:500; monoclonal 10D1; kindly provided by S. Piñol-Roma). Appropriate peroxidase-linked secondary antibodies (1:10,000; GE Healthcare UK Ltd.) were detected using SuperSignal West Dura (Pierce). To detect KIS in αKIS immunoprecipitates (IP), the eluted material was solubilized in the absence of 2-mercaptoethanol to avoid immunoglobulin G heavy-chain interference in the 50-kDa range during sodium dodecyl sulfate-polyacrylamide gel electrophoresis. In addition, anti-KIS antibodies used for Western detection were detected by sequential incubation with biotinylated protein A (1:1,000; Sigma) and peroxidase-linked streptavidin (1:1,000; Sigma). Chemiluminescence originated from Western blots was recorded with the aid of a charge-coupled-device-based camera (Lumimager; Roche), and the images were analyzed with the provided software to obtain accumulated pixel values for the indicated bands. To quantify immunoprecipitation efficiencies, NonO, KIF3A, and eEF1A levels were first made relative to the FLAG-KIS levels in the corresponding IP and then expressed as percentages of the values obtained with whole FLAG-KIS protein.

RNA in IP was extracted (RNeasy kit; Qiagen), treated with DNase I (Qiagen), and reverse transcribed with Superscript II reverse transcriptase (Invitrogen). The ratios of the several mRNAs tested to GAPDH (glyceraldehyde-3-phosphate dehydrogenase) mRNA were determined by quantitative real-time PCR using TaqMan probes for ACTB (*M. musculus* numbers are in parentheses) (00607939_s1), GRIA1 (00433753_m1), GRIA2 (00442822_m1), ARC (00479619_g1), MAPT (00521988_m1), MTAP2 (00485236_m1), NTRK2 (00435422_m1), TFRC (00441941_m1), CAMK2a (00437967_m1), SYAP1 (00481965_m1), PGAM1 (phosphoglycerate mutase 1) (02526975_g1), and GAPDH (99999915_g1) from Applied Biosystems. PCRs were run and analyzed with an iCycler iQ real-time detection system (Bio-Rad).

Isolation of RNA granules. The protocol for isolation of RNA granules was adapted from Kanai et al. (19). Lentivirus-infected cortical neurons were cultured for 7 days and homogenized in IMAC buffer (20 mM HEPES, pH 7.4, 140 mM potassium acetate, 1 mM magnesium acetate, 1 mM EGTA supplemented with protease inhibitors) containing 100 U/ml RNase inhibitor (Invitrogen) when indicated. The homogenate was fractionated by successive centrifugation steps to yield the indicated pellets (P) and supernatants (S). Total extracts were centrifuged at 1,000 × *g* for 10 min, giving rise to S1 and P1. The S1 supernatant was centrifuged at 10,000 × *g* for 10 min, yielding S2 and P2. The S2 supernatant was centrifuged at 100,000 × *g* for 1 h, resulting in S3 and P3. To investigate the effect of RNase, fraction S2 was incubated on ice for 2 h with 10 μg/ml RNase A (Amersham) prior to the last centrifugation.

Immunofluorescence, RNA staining, in situ hybridization, and live-cell imaging. One week after infection, cortical cells were quickly washed in phosphate-buffered saline (PBS) and fixed in 4% paraformaldehyde for 15 min at room temperature. The fixed cells were permeabilized with 0.5% Tween 20 in PBS for 2 min and blocked with 10% fetal calf serum for 30 min. Primary antibodies against HA (1:250; rat monoclonal 3F10; Roche) and KIF3A (1:250; monoclonal 28; BD Transduction Laboratory) were used in PBS with 1% fetal calf serum. Lentiviral HA-KIS levels were detected by sequential incubation with goat αrat and rabbit anti-goat antibodies labeled with Alexa 555 (1:500; Molecular Probes), while endogenous KIF3A was detected by incubation with an Alexa 488 rabbit anti-mouse antibody (1:500; Molecular Probes). For RNA staining, cells were incubated with 500 nM Syto14 for 15 min prior to fixation, and Alexa 647 secondary antibodies (Molecular Probes) were used for HA-KIS immunofluorescence. RNase treatment caused a severe reduction of Syto14 staining (data not shown). β-Actin mRNA detection by fluorescence in situ hybridization (FISH) in cortical neurons expressing HA-KIS was essentially as described previously (http://www.singerlab.org/protocols). The probes corresponded to positions in the rat β-actin mRNA chosen by Huttelmaier et al. (17): TXCAATGG GGTACTXCAGGGTCAGGAXACCTCTCTTGCXCTGGGCCTCGX, XGC CTGTGGXACGACCAGAGGCAXACAGGGACAGCACAGCCXGGATG GCX, XCAGCAATGCCXGGGTACATGGTGGXACCACCAGACAGCAC XGTGTTGGCAX, and AGGGXGAGGGACTTCCXGTAACCACTTAXTTC ATGGAXACTTGGAAXGAC, where X is amino-allyl C6-dT (DNA Technology A/S). Amino-allyl groups were labeled with Cy3 dye in 100 mM sodium

bicarbonate, pH 9.0, for 2 h at room temperature, as instructed by the manufacturer (Amersham), and the labeled probes were purified with Qiaex II (Qiagen). Following the hybridization and washing steps, HA-KIS was detected by immunofluorescence as described above with Alexa 488-labeled secondary antibodies (Molecular Probes). Images were acquired with an Olympus FV500 confocal system using a 60× objective on an Olympus IX81 inverted microscope. For in vivo fluorescence analysis, the medium was replaced with physiology buffer containing 119 mM NaCl, 2.5 mM KCl, 2 mM $CaCl_2$, 2 mM $MgCl_2$, 25 mM HEPES, pH 7.5, 30 mM glucose, and 100 nM BDNF, and the cells were kept at 37°C (DH-40i chamber; Warner) during observation for up to 30 min. Images were acquired using 20× and 40× objectives on an Olympus IX71 inverted microscope and DP manager software or 40× and 60× objectives on a Zeiss Axio Observer Z1 microscope and Axiovision 4.3 software.

Neurite length and single-cell expression analysis. Individual neuron tracings of GFP-expressing cells were measured using the NeuronJ plug-in developed by Erik Meijering for ImageJ (NIH) software. For each GFP-expressing cell, the number of neurites, the greatest neurite length, and the total neurite length were determined, and mean values per cell for each condition were obtained. For single-cell expression analysis using myr-dGFP$^{Actb\text{-}3'UTR}$ or GFP$^{Actb\text{-}3'UTR}$ (see below), images were acquired with parameters that maximized the range of pixel intensities for the neuritic signal. Identical acquisition parameters and settings were used for both control and experimental samples when their direct comparison was required. Using these parameters, the cell body fluorescence intensity was necessarily saturated. To prevent saturation, a different exposure time was used when the cell body DsRed fluorescence was analyzed. To analyze neuritic GFP$^{Actb\text{-}3'UTR}$ expression levels, we first eliminated the whole soma area from the fluorescence image using the freehand selection tool. Then, we obtained a baseline pixel value as a result of multiplying the image background by three, and the mean of the neuritic pixel intensity over the baseline value was calculated from pixel intensity histograms built by ImageJ. As expected (17, 41), raw fluorescence values obtained from GFP were ca. 20 times higher than those from GFP$^{Actb\text{-}3'UTR}$ in control cells. Prior to statistical analysis, the GFP fluorescence value for each cell was normalized to the mean value obtained from the respective control cells. A similar approach was used to determine and normalize DsRed levels in the neuronal soma. The relative values obtained were very similar for DsRed, DsRed-KIS, and DsRed-KIS^{KD} (data not shown), indicating that there were no major differences in transfection and expression efficiencies in independent experiments. To measure the fluorescence levels of myr-dGFP$^{Actb\text{-}3'UTR}$ particles, a macro was written in AxioVision 4.3 Commander to obtain the distance to soma and the total fluorescence for each particle. Levels of myr-dGFP$^{Actb\text{-}3'UTR}$ were determined by real-time RT-PCR as described above with a custom TaqMan probe (Applied Biosystems) (the coordinates relative to the *Zoanthus* sp. GFP ATG were 407 to 431 for the forward primer, 468 to 488 for the reverse primer, and 432 to 447 for the TaqMan probe).

RESULTS

KIS interacts with proteins of RNA granules. KIS is the only known protein kinase that possesses a U2AF homology motif (UHM), which is found immediately C-terminal to the kinase motif (KM) (Fig. 1A). Although the serine/threonine kinase domain has little homology to known kinases, a K54A^{KD} mutation in the putative active center of KIS ablates its kinase activity (28). The C-terminal region presents a 42% sequence similarity to U2AF65, a 65-kDa subunit of the splicing factor U2AF, which suggests that KIS could be involved in RNA-related processes. In order to explore putative interactions of KIS, we performed a yeast two-hybrid assay (Fig. 1B and C) to screen two mouse cDNA libraries (embryonic and adult brain) with full-length mouse KIS as bait. From the embryonic library, five clones carried full-length cDNA sequences coding for NonO, a protein implicated in a variety of nuclear processes, including transcription and mRNA splicing (20), and two clones encoding an N-terminal fragment (amino acids 48 to 257) of the protein biosynthesis elongation factor eEF1A. These two proteins have been identified in RNA-transporting granules purified from mouse brain (19). From the adult brain library, we isolated three clones encoding a C-terminal fragment (amino acids 448 to 702) of KIF3A, a microtubule-dependent motor protein abundantly expressed in the nervous system. The C-terminal domain of KIF3A is a region with no similarity to other kinesin-related proteins, and it has been proposed as a key determinant for specific interactions with KAP3 or PAR3, a protein involved in neuronal polarity (31). On the other hand, KIF3A has also been shown to be a component of Tau mRNA granules (3). Using two additional baits with different KIS moieties, we observed that interactions with KIF3A and NonO strictly required the N-terminal kinase domain of KIS (Fig. 1B and C). While the UHM was not essential, its deletion caused a significant reduction in the ability of KIS to interact with KIF3A and NonO. The yeast two-hybrid results were confirmed by coimmunoprecipitation experiments in HEK293T cells (Fig. 1D). The three proteins, KIF3A, NonO, and eEF1A, were able to interact with KISΔUHM but not with KISΔKM. Consistent with the two-hybrid assay as well, these interactions were weaker in cells expressing only the kinase domain (KISΔUHM) or a K54A^{KD} kinase-dead mutant (28) than in full-length KIS. These data indicate that the N-terminal domain of KIS is essential for the interaction with the identified proteins, while the C-terminal UHM may play a more indirect role through interaction with additional proteins and/or RNA or by conformational effects at the N-terminal domain. In addition, the kinase activity might be important to modulate the strength of the interactions.

KIS can be found in RNA granules. Since KIF3A, NonO, and eEF1A have previously been identified as components of neuronal RNA granules (3, 19), we explored the possibility that KIS was also localized in these RNA-transporting particles. As available anti-KIS antibodies were not sufficiently specific for immunofluorescence (see Materials and Methods), we used a lentiviral construct that expresses HA-KIS to levels very similar to endogenous KIS (Fig. 2B). Immunofluorescence with anti-HA antibodies revealed a punctate labeling pattern in both axon and dendrites. Figure 2A shows a representative example of a cortical neuron in which an important fraction of the HA-KIS signal colocalizes with RNA, as deduced from Syto14 labeling (24). Next, we performed subcellular fractionation by differential centrifugation of extracts from cortical neurons expressing FLAG-KIS. The distributions of FLAG-KIS, eEF1A, and KIF3A followed very similar patterns—all were RNase resistant—whereas the RNA binding proteins NonO, PSF, and hnRNP A/B disappeared from fraction P3 after RNase treatment (Fig. 2C). Thus, both KIS and KIF3A display behavior very similar to that of KIF5, which has been involved in transporting RNA granules to distal dendrites (19). KIS sedimentation properties were resistant to Triton X-100 (data not shown), making its association with vesicles unlikely. These results indicate that KIS would not require binding to RNA in order to localize to RNA granules, and they agree with the notion that UHM domains are optimized to interact with peptide ligands and may not directly bind RNA (22). Consistent with this, interactions of KIS with KIF3A, NonO, and eEF1A in HEK293T cells were unaffected by RNase treatment (Fig. 1E). Thus, KIS would associate directly with RNP components, such as KIF3A, eEF1A, or NonO, whether they bind to RNA or not. We next examined whether HA-KIS was found associated with the kinesin KIF3A in neurites. Figure 2D shows that the majority of HA-KIS granules included endog-

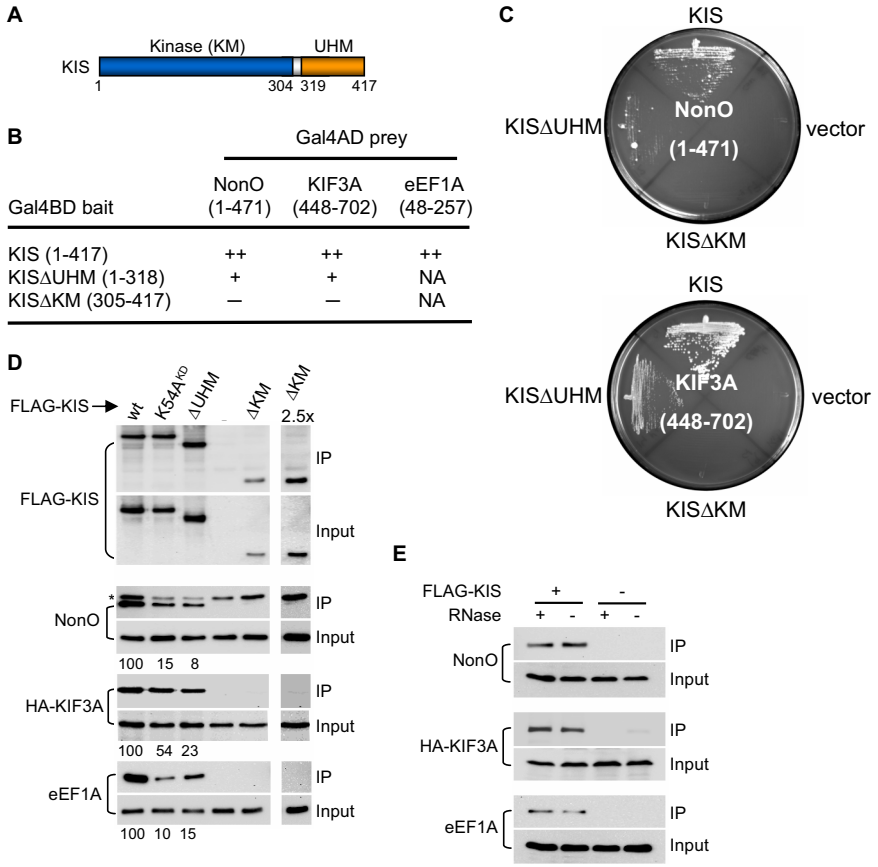

FIG. 1. Interactions of KIS with NonO, KIF3A, and eEF1A in the yeast two-hybrid assay and HEK293T cells. (A) Domain structure of KIS. The numbers refer to amino acids. (B) Two-hybrid interactions of full-length KIS and versions that lack the kinase domain (KISΔKM) or the UHM domain (KISΔUHM) with NonO, KIF3A, and eEF1A. Residues present in bait constructs, as well as positive clones isolated from prey libraries, are shown in parentheses. Full (++), partial (+), and no (−) complementation for growth are indicated. (C) Cells were plated in synthetic complete medium without histidine in the presence of 25 mM aminotriazole and incubated at 30°C for 3 days. (D) HEK293T cells expressing FLAG-tagged versions of full-length KIS (wt), a kinase-dead mutant ($K54A^{KD}$), kinase domain (ΔUHM), UHM domain (ΔKM), or empty vector (−) as a negative control were used for immunoprecipitation with anti-FLAG antibody. The input and anti-FLAG IP were analyzed by Western blotting to detect endogenous NonO and eEF1A or cotransfected HA-KIF3A and FLAG-KIS proteins. The amounts of NonO, HA-KIF3A, and eEF1A proteins in IP were quantitated, and data relative to the respective immunoprecipitated FLAG-KIS proteins are indicated. NonO, HA-KIF3A, and eEF1A were barely detectable in ΔKM IP even after the exposure time was increased 2.5-fold. An immunoglobulin G cross-reactive band is indicated by an asterisk. (E) HEK293T cells expressing FLAG-KIS or transfected with empty vector (−) as a negative control were used for immunoprecipitation with anti-FLAG antibody as described above. Extracts were incubated on ice for 2 h with 10 μg/ml RNase A (+) or 100 U/ml RNase inhibitor (−) prior to immunoprecipitation. The input and anti-FLAG IP were analyzed by Western blotting to detect endogenous NonO and eEF1A or cotransfected HA-KIF3A and FLAG-KIS proteins.

enous KIF3A, indicating that the two proteins might be present in a specific set of RNA granules. Thus, our results suggest that neuritic transport of KIS-containing granules involves the motor protein KIF3A, most likely through a direct interaction with the C-terminal tail of the kinesin.

KIS is required for neuritic outgrowth. KIS is expressed mainly in adult neural tissues, and its expression increases during brain development (28). To determine whether KIS has a relevant role in neuronal function, we tested the effects of KIS knockdown by siRNA as described previously (Fig. 3A) (5). Differentiated cells were cotransfected with a GFP reporter vector and either control or KIS siRNA (Fig. 3B). Cells treated with KIS siRNA showed a clear reduction in total neuritic length and the neurite count per cell (Fig. 3C and D) at 16 h after transfection. At later times, 24 h after transfection, we observed a twofold increase in the percentage of picnotic nuclei in cells transfected with KIS siRNA compared to the siRNA control (data not shown). These results suggest that KIS has an essential function for neurite outgrowth in cortical neurons. KIF3A has been shown to be required for neurite outgrowth in P19 cells (3), reinforcing the notion that the two proteins could have related roles in neurite development and/or maintenance.

KIS associates with KIF3A and RNP-transported mRNAs in whole-brain extracts. To strengthen the idea that KIS is found associated with KIF3A in neurons, we used whole-brain extracts from newborn mice to immunoprecipitate endogenous KIS with a polyclonal antibody (5). As shown in Fig. 4A, we were able to detect a small fraction of KIF3A in the anti-KIS IP, thus confirming the interaction between the two proteins. On the other hand, we were not able to detect KIS in the

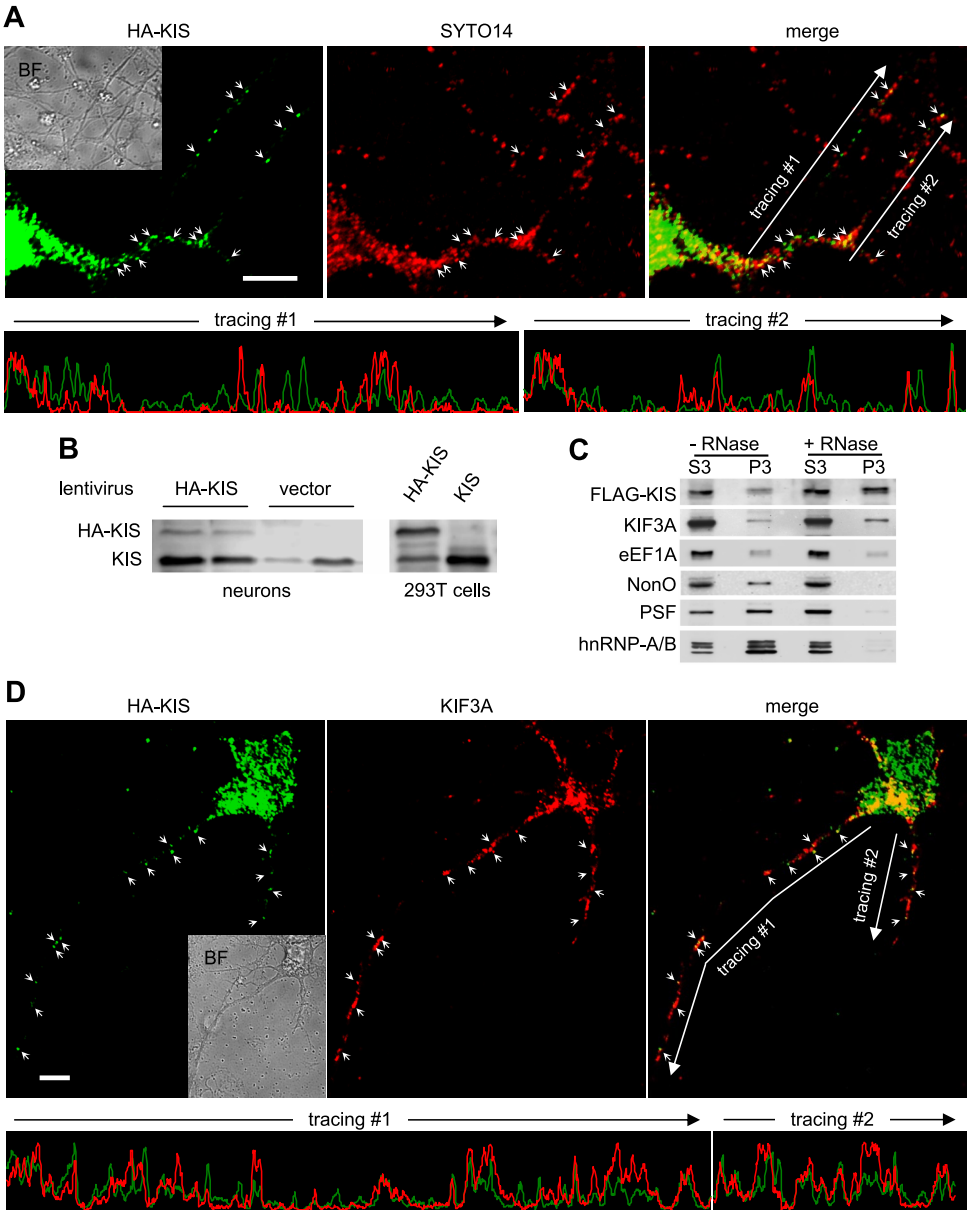

FIG. 2. KIS colocalizes with RNA and KIF3A. (A) Cortical neurons infected with a lentiviral vector expressing HA-KIS were labeled with Syto14 to detect RNA and analyzed by immunofluorescence with an anti-HA antibody. Bar, 5 μm. The inset shows a reduced bright-field image. Profiles of HA-KIS (green) and Syto14 (red) fluorescence values are shown for the indicated tracings. (B) Western blot analysis of endogenous KIS and lentiviral HA-KIS proteins expressed by cortical neurons. In this experiment, the infection efficiency was ca. 27%, as deduced from immunofluorescence analysis. Lentiviral HA-KIS and endogenous KIS protein levels attained in HEK293T cells are also shown. (C) Subcellular fractionation of cortical cells expressing FLAG-KIS. The final supernatant (S3) and pellets (P3), incubated with (+) or without (−) RNase prior to the last centrifugation, were analyzed by Western blotting with antibodies against KIF3A, eEF1A, NonO, PSF, and hnRNP A/B proteins. FLAG-KIS and NonO proteins were expressed from lentiviral vectors and detected with anti-FLAG and anti-NonO antibodies. (D) Cortical neurons were analyzed by immunofluorescence to detect lentiviral HA-KIS and endogenous KIF3A proteins. Bar, 5 μm. The inset shows a reduced bright-field image. Profiles of HA-KIS (green) and KIF3A (red) fluorescence values are shown for the indicated tracings.

anti-KIF3A IP, likely as a result of the very low efficiency at which KIF3A was immunoprecipitated with the available antibody. Next, we analyzed anti-KIS IP by real-time RT-PCR to evaluate the presence of a number of mRNAs that are known or proposed to be transported along axons and/or dendrites. Figure 4B shows that the β-actin mRNA was found to be moderately enriched relative to the GAPDH mRNA in anti-KIS IP. Notably, almost all other mRNAs tested were enriched more than fourfold in anti-KIS IP. As an additional control, levels of the mRNA coding for PGAM1 were very similar to those corresponding to the GAPDH mRNA in all IP. Finally, the plotted values in Fig. 4 are the means of three independent IP experiments that gave comparable results (data not shown). Our data suggest that KIS could associate at different efficiencies with RNPs with distinct mRNAs, which could explain in part why KIS is not present in all RNA particles, as detected by

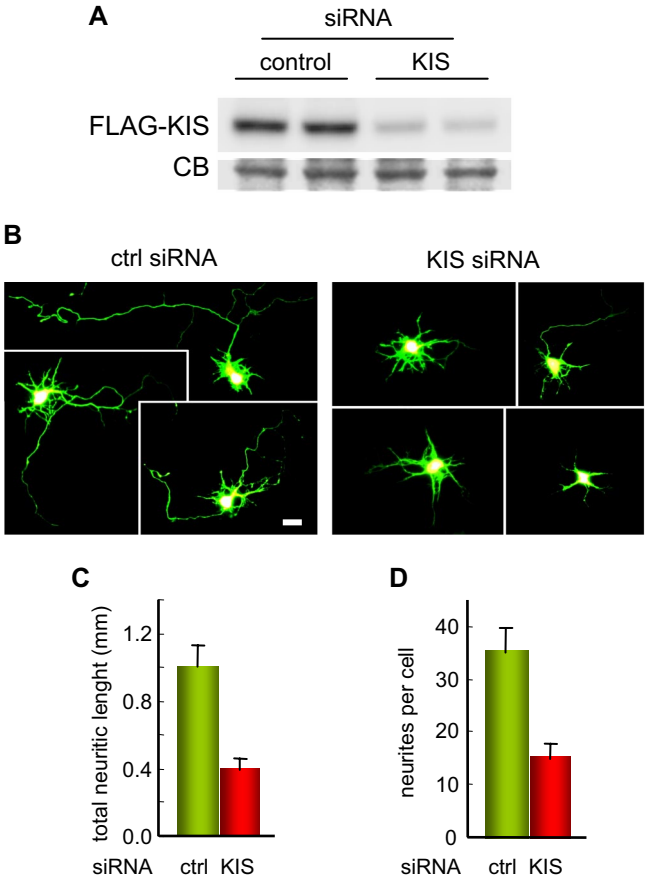

FIG. 3. KIS plays a relevant role in neuritic outgrowth. (A) HEK293T cells were cotransfected with FLAG-KIS and either KIS siRNA or a scrambled control siRNA. Samples were analyzed by Western blotting to detect FLAG-KIS. The corresponding region of the blot stained with Coomassie blue (CB) is shown as a loading control. (B) Cortical neurons were cotransfected with a GFP reporter vector and either control or KIS siRNA and analyzed 16 h after transfection. Representative cells are shown for each condition. Bar, 20 μm. (C and D) Mean values and confidence limits ($\alpha = 0.01$) for the total neurite length per cell (C) and the number of neurites longer than 3 μm in each cell (D) were plotted.

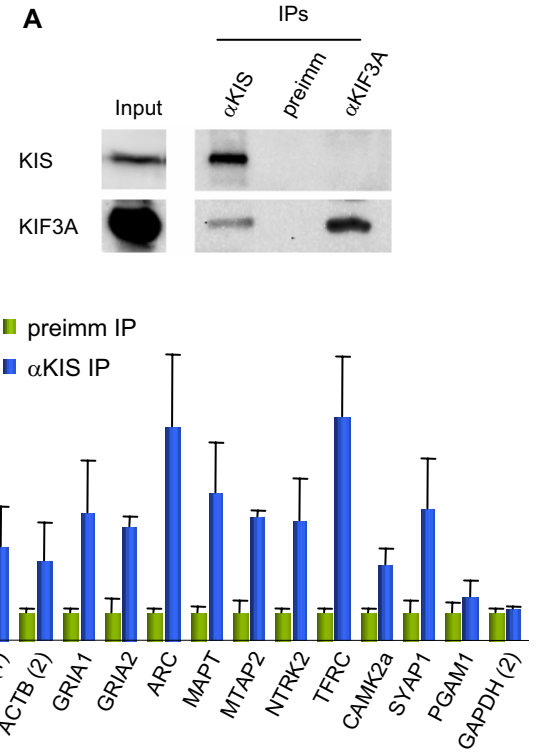

FIG. 4. KIS interacts with KIF3A and RNP-transported mRNAs in postnatal brain extracts. (A) Whole brains from newborn mice were used in immunoprecipitation assays with anti-KIS, anti-KIF3A, or preimmune antisera. IP and a sample corresponding to 1/200 of the input were analyzed by Western blotting to detect endogenous KIS and KIF3A proteins. (B) IP with anti-KIS and the preimmune (preimm) antisera shown in panel A were used to quantify the relative levels of the indicated mRNAs by real-time RT-PCR. Gene symbols and descriptions are as follows: ACTB, β-actin, cytoplasmic; GRIA1, glutamate receptor, ionotropic, AMPA1 (alpha 1); GRIA2, glutamate receptor, ionotropic, AMPA2 (alpha 2); ARC, activity-regulated cytoskeletal-associated protein; MAPT, microtubule-associated protein Tau; MTAP2, microtubule-associated protein 2; NTRK2, neurotrophic tyrosine kinase, receptor TrkB, type 2; TFRC, transferrin receptor; CAMK2a, calcium/calmodulin-dependent protein kinase II alpha; SYAP1, synapse-associated protein 1. Ratios to GAPDH mRNA were obtained, and the mean values from three independent immunoprecipitation experiments and respective confidence limits ($\alpha = 0.05$) were plotted. In addition, two sets of independent data were obtained for β-actin mRNA (ACTB). PGAM1 and a second measurement for GAPDH (2) were included as controls.

Syto14 staining. More importantly, as they were identified with endogenous proteins, these KIS-KIF3A and KIS-mRNA interactions underline the functional relevance of KIS in vivo.

KIS colocalizes with β-actin mRNA in cortical neurons. As the distribution of KIS in neurites is very similar to that described for the β-actin mRNA in embryonic cortical cells and neuroblastoma cell lines (17, 38), we decided to analyze the localization of the β-actin mRNA by FISH and that of HA-KIS by immunofluorescence in cortical neurons. Similarly to ZBP1 (17), KIS colocalized with β-actin mRNA at the leading edge and along neurites of cortical neurons (Fig. 5A). In agreement with the results obtained with whole-brain extracts, we found that the β-actin mRNA was also significantly enriched compared to GAPDH mRNA in FLAG-KIS IP, as deduced from real-time RT-PCR analysis (Fig. 5B and C).

KIS enhances translation driven by the β-actin 3′ UTR. An important aspect of mRNA localization involves the inhibition of mRNA expression until it is activated by specific synaptic inputs (37). Huttelmaier and colleagues have showed that local control of β-actin protein levels is essential for proper neurite outgrowth and neuronal differentiation (17). In order to test whether KIS is functionally related to local translation, we used $GFP^{Actb\text{-}3'UTR}$, a GFP fusion to the 3′ UTR of the β-actin mRNA. As expected from its inhibitory effect on translation (17, 41), fusing the β-actin 3′ UTR to GFP caused an important reduction (to ca. 5%) in its overall expression levels. Thus, cortical neurons were cotransfected with GFP or $GFP^{Actb\text{-}3'UTR}$ and with DsRed and DsRed fusions to KIS and the KIS^{KD} mutant, and images were obtained 14 to 16 h after transfection (Fig. 6A) for single-cell expression analysis (see Materials and Methods for details). Figure 6B shows that KIS stimulated neuritic $GFP^{Actb\text{-}3'UTR}$ levels but not those of control GFP. In

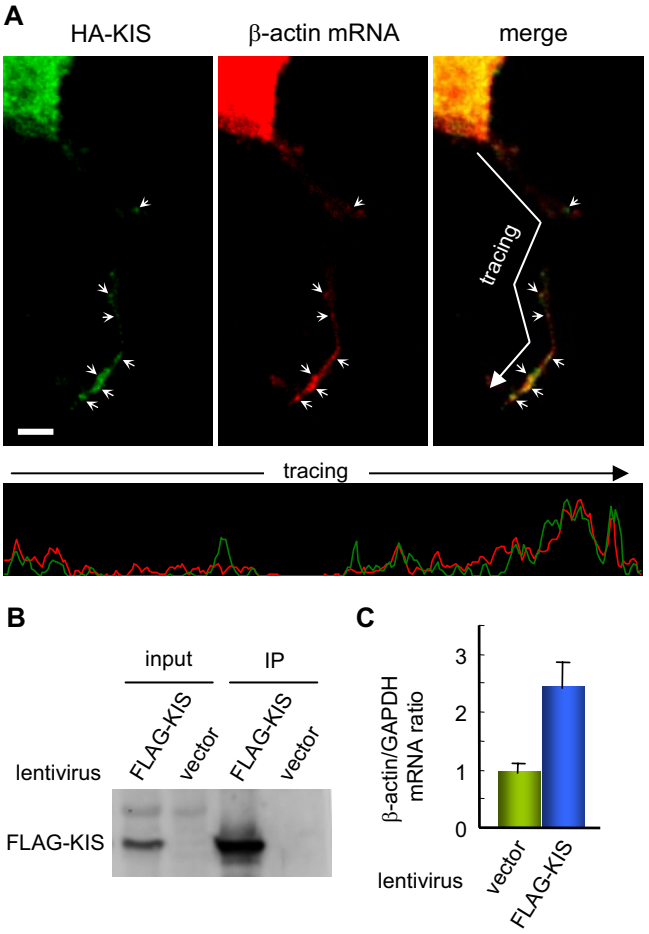

FIG. 5. KIS colocalizes and associates with β-actin mRNA in cortical neurons. (A) Cortical neurons expressing HA-KIS were analyzed by FISH with a β-actin mRNA probe and subsequently processed for immunofluorescence with an anti-HA antibody. Bar, 5 μm. Profiles of HA-KIS (green) and β-actin mRNA (red) fluorescence values are shown for the indicated tracing. (B) Input extracts and αFLAG IP from cortical neurons infected with a FLAG-KIS lentiviral construct or the empty vector were analyzed by Western blotting. (C) IP shown in panel B were used to determine β-actin/GAPDH mRNA ratios by real-time RT-PCR. The mean values of six measurements from three independent experiments and the respective confidence limits (α = 0.05) were plotted.

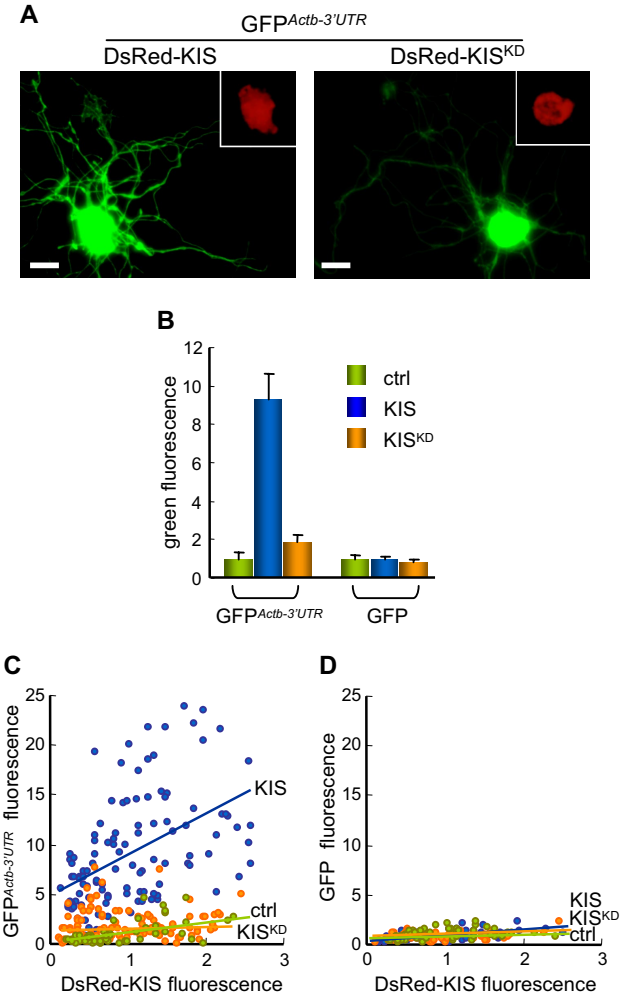

FIG. 6. KIS overexpression increases neuritic GFP$^{Actb\text{-}3'UTR}$ levels in a kinase-dependent manner. (A) In vivo fluorescence images of two representative neurons cotransfected with GFP$^{Actb\text{-}3'UTR}$ and DsRed fusions to KIS or the KIS^{KD} mutant, which are shown in the corresponding insets as short-exposure images to observe only the red signal in soma. Bars, 10 μm. (B) Fourteen to 16 h after transfection with GFP$^{Actb\text{-}3'UTR}$ or GFP-expressing vectors and either DsRed-, DsRed-KIS-, or DsRed-KIS^{KD}-expressing constructs, green fluorescence in neurites and red fluorescence in soma were quantified and normalized to those of DsRed cells. The mean values ($n \geq 50$) and confidence limits for the mean (α = 0.01) are plotted. ctrl, control. (C) Correlation analysis between normalized values of neuritic GFP$^{Actb\text{-}3'UTR}$ and normalized values of somatic DsRed, DsRed-KIS, and DsRed-KIS^{KD} levels in the transfected cells analyzed in panel B. (D) Correlation analysis for neuritic GFP signal as in panel C.

contrast, KIS^{KD} was not able to increase neuritic GFP$^{Actb\text{-}3'UTR}$ levels compared to the control, indicating that the kinase activity of KIS is essential to stimulate neuritic accumulation of GFP$^{Actb\text{-}3'UTR}$. Furthermore, a positive correlation was observed between the neuritic GFP$^{Actb\text{-}3'UTR}$ signal and the DsRed-KIS level in soma (Fig. 6C) that was not observed in DsRed-KIS^{KD}-transfected cells or DsRed-transfected control cells (Fig. 6C). Finally, no correlation was observed with any of the DsRed constructs when cotransfected with control GFP (Fig. 6D), which demonstrated the specific dependence on the β-actin 3′ UTR and suggested that KIS is not a general activator of translation. In order to avoid cumulative effects of GFP expression, we used a destabilized version of *Zoanthus* sp. GFP fused to a myristoylation consensus sequence at the N terminus (myr-dGFP$^{Actb\text{-}3'UTR}$) to confer membrane localization and limit protein diffusion (1). In contrast to conventional GFP, the myr-dGFP$^{Actb\text{-}3'UTR}$ protein produced a punctate pattern (Fig. 7A). To discard possible transcriptional or mRNA stability effects, we measured GFP mRNA levels by real-time RT-PCR and found that they were not significantly altered by cotransfection with vectors expressing DsRed-KIS or DsRed-KIS^{KD} compared to the DsRed control (Fig. 7B). Indeed, the fluorescence level of myr-dGFP$^{Actb\text{-}3'UTR}$ particles in DsRed-KIS-expressing cells showed a fivefold increase compared to control cells ex-

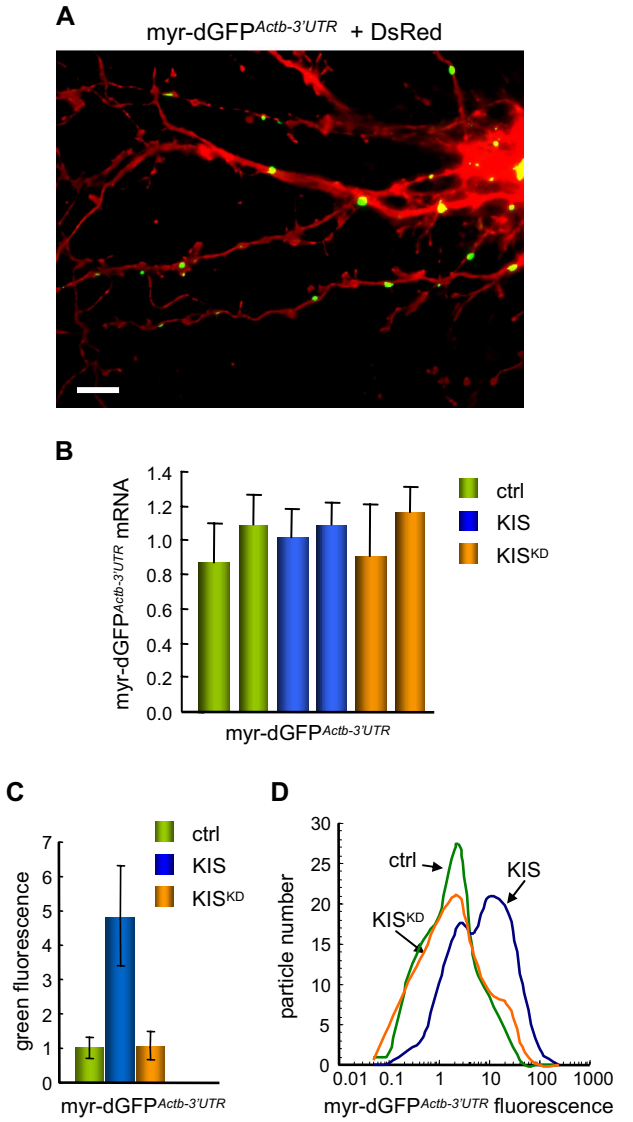

FIG. 7. KIS overexpression stimulates myr-dGFP$^{Actb\text{-}3'UTR}$ expression levels in neurites. (A) In vivo fluorescence image of a representative cell cotransfected with myr-dGFP$^{Actb\text{-}3'UTR}$ and DsRed. Bar, 5 μm. (B, C, and D) Cortical neurons were cotransfected with myr-dGFP$^{Actb\text{-}3'UTR}$ and either DsRed-, DsRed-KIS-, or DsRed-KIS^{KD}-expressing constructs and incubated for 14 to 16 h. The levels of myr-dGFP$^{Actb\text{-}3'UTR}$ mRNA were determined by real-time RT-PCR analysis from equivalent amounts of total RNA, and the mean values and confidence limits ($\alpha = 0.05$) from three measurements of two independent experiments are plotted (B). The total fluorescence in myr-dGFP$^{Actb\text{-}3'UTR}$ particles ($n > 650$) was quantified as described in Materials and Methods. Median values with confidence limits ($\alpha = 0.05$) (C) and logarithmic distributions (D) were plotted. ctrl, control.

pressing DsRed or DsRed-KIS^{KD} (Fig. 7C). This increase was observed in most particles of the analyzed population (Fig. 7D). On the other hand, the number of myr-dGFP$^{Actb\text{-}3'UTR}$ particles per cell and their distance to soma was not significantly affected by KIS overexpression (data not shown). Thus, our findings underline the physiological relevance of the kinase activity of KIS and support the notion that KIS acts as a modulator of local translation in cortical neurons.

DISCUSSION

The serine/threonine kinase KIS was initially identified as a protein interacting with stathmin in a two-hybrid system (27), and its expression pattern suggested a role in the developing nervous system and the adult brain (4). KIS has been shown to phosphorylate p27^{Kip1} and to control its subcellular localization, indicating an important role as a regulator of cell cycle progression (5). While the kinase domain of KIS shows no compelling homology with those of other kinases, the C-terminal region presents a 42% sequence similarity to the splicing factor U2AF65. In this sense, KIS has been shown to phosphorylate SF1, a spliceosome assembly factor (29). In the present study, we show that KIS interacts with KIF3A, NonO, and eEF1A, three proteins known to be present in RNA granules (34). The N-terminal domain of KIS is essential for efficient binding to the three proteins, while a kinase-dead mutant showed weaker interactions, which suggests that the kinase activity could modulate the interaction between KIS and components of the RNA granule.

Motor proteins are composed of a head domain with ATPase activity used for microtubule binding, whereas the C-terminal tail contains the cargo-binding domains (15). In this regard, the kinase CamKIIα has been shown to phosphorylate the KIF17 kinesin in its C-terminal region, causing dissociation of Mint1, a protein that links the kinesin with its vesicle cargo. Thus, kinesin phosphorylation would unload the transported cargo in the vicinity of the synapse (13). Our results suggest that neuritic transport of KIS-containing granules involves the motor protein KIF3A, most likely through a direct interaction with its C-terminal tail, as deduced from our two-hybrid screen. Since KIS does not phosphorylate KIF3A in vitro (our unpublished results), KIS could phosphorylate other proteins mediating the interaction between the kinesin and its cargo to release the RNA granule at proper sites.

The notion that mRNAs acquire in the nucleus their competence to be specifically sorted in the cytoplasm has been recently strengthened in neurons. Thus, proteins involved in splicing processes, such as hnRNPs, SRs, PSF, or NonO, are also found in RNA granules (19), and several components of the exon junction complex have a role in local mRNA translation, as well (10, 14, 25). Related to these results, KIS has been shown to phosphorylate the spliceosome assembly factor SF1 (29), and we have observed that KIS interacts with NonO and colocalizes with the splicing factor SC35 in nuclear speckles in COS-7 cells (our unpublished results), which suggests that KIS could be recruited to RNP complexes in the nucleus and perform additional essential functions in cortical neurons.

A central emerging theme in the field of dendritic regulation is the possibility of reciprocal interactions between actin dynamics and dendritic protein synthesis in the control of synaptic plasticity (6). A large percentage of ribosomes associate with F-actin in neurons, and microfilament association is necessary for translation from specific RNA granules. The elongation factor eEF1A is known to promote actin bundling independently of its function in translation elongation (8, 26). A recent study of yeast showed that mutations of the actin interaction

region of eEF1A led to improper organization of the actin cytoskeleton and translation inhibition at initiation (not elongation) (11, 12). These findings strongly support a role for eEF1A in assembling actin filaments into a compartment to which mRNA becomes anchored and translated. Finally, phosphorylation of eEF1A in a primary culture of rat cortical neurons treated with BDNF has been shown to be correlated with an increase in translational activity (18, 36). However, as KIS does not phosphorylate eEF1A in vitro (our unpublished results), KIS could phosphorylate other associated proteins to release eEF1A from the actin cytoskeleton and/or increase its activity to enhance local translation of target mRNAs. Accordingly, we show here that KIS stimulates the expression of two different GFP reporter fusions to the β-actin 3′ UTR, and this effect is strictly dependent on the kinase activity of KIS. No effect was observed in the absence of the β-actin 3′ UTR, indicating that KIS does not act as a general activator of translation. We have found that KIS colocalizes with β-actin mRNA with a pattern similar to what has been reported for β-actin mRNA and protein (40). On the other hand, translation of β-actin in the growth cone is essential for neurite extension. Thus, delocalization of the β-actin mRNA, which causes a decrease of β-actin protein levels at the leading edges of the growth cone, results in growth cone retraction and nondirectional growth cone guidance (41). Accordingly, we have found that KIS knockdown causes a strong reduction in the total neuritic length and in the number of neurites per cell in cortical neurons. These results suggest that KIS has an essential role in neuritogenesis, modulating local translation of β-actin mRNA and other RNP-transported mRNAs (7).

Src kinase phosphorylates ZBP1 to relieve β-actin mRNA translation inhibition (17), suggesting that Src could be a trigger factor transmitting local signals originating from tyrosine kinase receptors, such as TrkB. We have compared the KIS sequence with sequences of ZBP1 and other Src targets and found that KIS contains putative phosphorylation and docking sites for Src. We hypothesize that KIS could serve to transmit local Src activation and to phosphorylate additional targets in the RNA granule, thus amplifying the signal and providing further specificity effects. As we discuss above, once activated by Src, KIS could phosphorylate associated proteins to release the RNA granule and stimulate translation elongation at the proper sites. In addition, activation of the kinase activity of KIS would increase its affinity for eEF1A and, to a lesser extent, KIF3A, which should also contribute to the local amplification of the signal. Future studies will be necessary to identify the targets of KIS and to determine the mechanism by which it regulates local expression in neurons.

ACKNOWLEDGMENTS

We thank I. Navarro and S. Rius for technical assistance and M. Encinas and S. Piñol for the gift of antibodies. We also thank M. Encinas, J. Esquerda, E. Izaurralde, R. H. Singer, J. Valcárcel, and C. Vicario for helpful comments and N. Colomina and J. Torres for critically reading the manuscript.

This work was supported by the Ministry of Education and Science of Spain, Consolider-Ingenio 2010, Fundació La Caixa, and the European Union (FEDER). N.P. is a researcher of the Juan de la Cierva program.

REFERENCES

1. **Aakalu, G., W. B. Smith, N. Nguyen, C. Jiang, and E. M. Schuman.** 2001. Dynamic visualization of local protein synthesis in hippocampal neurons. Neuron **30:**489–502.
2. **Anderson, P., and N. Kedersha.** 2006. RNA granules. J. Cell Biol. **172:**803–808.
3. **Aronov, S., G. Aranda, L. Behar, and I. Ginzburg.** 2002. Visualization of translated tau protein in the axons of neuronal P19 cells and characterization of tau RNP granules. J. Cell Sci. **115:**3817–3827.
4. **Bièche, I., V. Manceau, P. A. Curmi, I. Laurendeau, S. Lachkar, K. Leroy, D. Vidaud, A. Sobel, and A. Maucuer.** 2003. Quantitative RT-PCR reveals a ubiquitous but preferentially neural expression of the KIS gene in rat and human. Brain Res. Mol. Brain Res. **114:**55–64.
5. **Boehm, M., T. Yoshimoto, M. F. Crook, S. Nallamshetty, A. True, and G. E. Nabel.** 2002. A growth factor-dependent nuclear kinase phosphorylates p27(Kip1) and regulates cell cycle progression. EMBO J. **21:**3390–3401.
6. **Bramham, C. R., and D. G. Wells.** 2007. Dendritic mRNA: transport, translation and function. Nat. Rev. Neurosci. **8:**1–14.
7. **Condeelis, J., and R. H. Singer.** 2005. How and why does beta-actin mRNA target? Biol. Cell **97:**97–110.
8. **Edmonds, B. T., J. Wyckoff, Y. G. Yeung, Y. Wang, E. R. Stanley, J. Jones, J. Segall, and J. Condeelis.** 1996. Elongation factor-1α is an overexpressed actin-binding protein in metastatic rat mammary adenocarcinoma. J. Cell Sci. **109:**2705–2714.
9. **Elvira, G., S. Wasiak, V. Blandford, X. K. Tong, A. Serrano, X. Fan, M. del Rayo Sanchez-Carbente, F. Servant, A. W. Bell, D. Boismenu, J. C. Lacaille, P. S. McPherson, L. DesGroseillers, and W. S. Sossin.** 2006. Characterization of an RNA granule from developing brain. Mol. Cell. Proteomics **5:**635–651.
10. **Giorgi, C., G. W. Yeo, M. E. Stone, D. B. Katz, C. Burge, G. Turrigiano, and M. J. Moore.** 2007. The EJC factor eIF4AIII modulates synaptic strength and neuronal protein expression. Cell **130:**179–191.
11. **Gross, S. R., and T. G. Kinzy.** 2005. Translation elongation factor 1A is essential for regulation of the actin cytoskeleton and cell morphology. Nat. Struct. Mol. Biol. **12:**772–778.
12. **Gross, S. R., and T. G. Kinzy.** 2007. Improper organization of the actin cytoskeleton affects protein synthesis at initiation. Mol. Cell. Biol. **27:**1974–1989.
13. **Guillaud, L., R. Wong, and N. Hirokawa.** 2008. Disruption of KIF17-Mint1 interaction by CaMKII-dependent phosphorylation, a molecular model of kinesin-cargo release. Nat. Cell Biol. **1:**19–29.
14. **Hachet, O., and A. Ephrussi.** 2004. Splicing of oskar RNA in the nucleus is coupled to its cytoplasmic localization. Nature **428:**959–963.
15. **Hirokawa, N., and R. Takemura.** 2005. Molecular motors and mechanisms of directional transport in neurons. Nat. Rev. Neurosci. **6:**201–214.
16. **Huang, Y. S., J. H. Carson, E. Barbarese, and J. D. Richter.** 2003. Facilitation of dendritic mRNA transport by CPEB. Genes Dev. **17:**638–653.
17. **Huttelmaier, S., D. Zenklusen, M. Lederer, J. Dictenberg, M. Lorenz, X. Meng, G. J. Bassell, J. Condeelis, and R. H. Singer.** 2005. Spatial regulation of β-actin translation by Src-dependent phosphorylation of ZBP1. Nature **438:**512–515.
18. **Inamura, N., H. Nawa, and N. Takei.** 2005. Enhancement of translation elongation in neurons by brain-derived neurotrophic factor: implications for mammalian target of rapamycin signaling. J. Neurochem. **95:**1438–1445.
19. **Kanai, Y., N. Dohmae, and N. Hirokawa.** 2004. Kinesin transports RNA, isolation and characterization of an RNA-transporting granule. Neuron **43:**513–525.
20. **Kaneko, S., O. Rozenblatt-Rosen, M. Meyerson, and J. L. Manley.** 2007. The multifunctional protein p54nrb/PSF recruits the exonuclease XRN2 to facilitate pre-mRNA 3′ processing and transcription termination. Genes Dev. **21:**1779–1789.
21. **Kiebler, M. A., and G. J. Bassell.** 2006. Neuronal RNA granules, movers and makers. Neuron **51:**685–690.
22. **Kielkopf, C. L., S. Lucke, and M. R. Green.** 2004. U2AF homology motifs, protein recognition in the RRM world. Genes Dev. **18:**1513–1526.
23. **Kindler, S., H. Wang, D. Richter, and H. Tiedge.** 2005. RNA transport and local control of translation. Annu. Rev. Cell Dev. Biol. **21:**223–245.
24. **Knowles, R. B., J. H. Sabry, M. E. Martone, T. J. Deerinck, M. H. Ellisman, G. J. Bassell, and K. S. Kosik.** 1996. Translocation of RNA granules in living neurons. J. Neurosci. **16:**7812–7820.
25. **Le Hir, H., D. Gatfield, I. C. Braun, D. Forler, and E. Izaurralde.** 2001. The protein Mago provides a link between splicing and mRNA localization. EMBO Rep. **12:**1119–1124.
26. **Liu, G., W. M. Grant, D. Persky, V. M. Latham, Jr., R. H. Singer, and J. Condeelis.** 2002. Interactions of elongation factor 1α with F-actin and β-actin mRNA: implications for anchoring mRNA in cell protrusions. Mol. Biol. Cell **13:**579–592.
27. **Maucuer, A., J. P. Le Caer, V. Manceau, and A. Sobel.** 2000. Specific Ser-Pro phosphorylation by the RNA-recognition motif containing kinase KIS. Eur. J. Biochem. **267:**4456–4464.
28. **Maucuer, A., S. Ozon, V. Manceau, O. Gavet, S. Lawler, P. Curmi, and A.**

Sobel. 1997. KIS is a protein kinase with an RNA recognition motif. J. Biol. Chem. **272:**23151–23156.
29. **Manceau, V., M. Swenson, J. P. Le Caer, A. Sobel, C. L. Kielkopf, and A. Maucuer.** 2006. Major phosphorylation of SF1 on adjacent Ser-Pro motifs enhances interaction with U2AF65. FEBS J. **273:**577–587.
30. **Mori, Y., K. Imaizumi, T. Katayama, T. Yoneda, and M. Tohyama.** 2000. Two *cis*-acting elements in the 3′ untranslated region of α-CaMKII regulate its dendritic targeting. Nat. Neurosci. **3:**1079–1084.
31. **Nishimura, T., K. Kato, T. Yamaguchi, Y. Fukata, S. Ohno, and K. Kaibuchi.** 2004. Role of the PAR-3-KIF3 complex in the establishment of neuronal polarity. Nat. Cell Biol. **6:**328–334.
32. **Rodriguez, A. J., K. Czaplinski, J. S. Condeelis, and R. H. Singer.** 2008. Mechanisms and cellular roles of local protein synthesis in mammalian cells. Curr. Opin. Cell Biol. **127:**49–58.
33. **Sonenberg, N., and A. G. Hinnebusch.** 2007. New modes of translational control in development, behavior, and disease. Mol. Cell **28:**721–729.
34. **Sossin, W. S., and L. DesGroseillers.** 2006. Intracellular trafficking of RNA in neurons. Traffic **7:**1581–1589.
35. **St Johnston, D.** 2005. Moving messages: the intracellular localization of mRNAs. Nat. Rev. Mol. Cell Biol. **6:**363–375.
36. **Sutton, M. A., and E. M. Schuman.** 2005. Local translational control in dendrites and its role in long-term synaptic plasticity. J. Neurobiol. **64:**116–131.
37. **Sutton, M. A., and E. M. Schuman.** 2006. Dendritic protein synthesis, synaptic plasticity, and memory. Cell **127:**49–58.
38. **Tiruchinapalli, D. M., Y. Oleynikov, S. Kelic, S. M. Shenoy, A. Hartley, P. K. Stanton, R. H. Singer, and G. J. Bassell.** 2003. Activity-dependent trafficking and dynamic localization of zipcode binding protein 1 and β-actin mRNA in dendrites and spines of hippocampal neurons. J. Neurosci. **23:**3251–3261.
39. **Watabe-Uchida, M., K. A. John, J. A. Janas, S. E. Newey, and L. Van Aelst.** 2006. The Rac activator DOCK7 regulates neuronal polarity through local phosphorylation of stathmin/Op18. Neuron **51:**727–739.
40. **Zhang, H. L., R. H. Singer, and G. J. Bassell.** 1999. Neurotrophin regulation of beta-actin mRNA and protein localization within growth cones. J. Cell Biol. **147:**59–70.
41. **Zhang, H. L., T. Eom, Y. Oleynikov, S. M. Shenoy, D. A. Liebelt, J. B. Dictenberg, R. H. Singer, and G. J. Bassell.** 2001. Neurotrophin-induced transport of a beta-actin mRNP complex increases beta-actin levels and stimulates growth cone motility. Neuron **31:**261–275.